Fire regime impacts on postfire diurnal land surface temperature change over North American boreal forest

Jie Zhao, Liang Wang, Xin Hou, Guangyao Li, Qi Tian, Eme Chan, Philippe Ciais, Qiang Yu, Chao Yue

JGR Atmospheres

RESEARCH ARTICLE
10.1029/2021JD035589

Fire Regime Impacts on Postfire Diurnal Land Surface Temperature Change Over North American Boreal Forest

Jie Zhao[1], Liang Wang[2], Xin Hou[1], Guangyao Li[1], Qi Tian[1], Eme Chan[3], Philippe Ciais[4], Qiang Yu[5,6,7], and Chao Yue[1,5,8]

[1]College of Natural Resources and Environment, Northwest A&F University, Yangling, China, [2]Shandong Provincial Key Laboratory of Water and Soil Conservation and Environmental Protection, College of Resources and Environment, Linyi University, Linyi, China, [3]School of Public Administration, China University of Geosciences (Wuhan), Wuhan, China, [4]Laboratoire des Sciences du Climat et de l'Environnement, CEA-CNRS-UVSQ, Gif sur Yvette, France, [5]State Key Laboratory of Soil Erosion and Dryland Farming on the Loess Plateau, Northwest A&F University, Yangling, China, [6]School of Life Sciences, University of Technology Sydney, Sydney, NSW, Australia, [7]Key Laboratory of Water Cycle and Related Land Surface Processes, Institute of Geographic Sciences and Natural Resources Research, Chinese Academy of Sciences, Beijing, China, [8]College of Forestry, Northwest A&F University, Yangling, China

Key Points:

- Forest fires cause surface warming during daytime but cooling at night
- Fire regimes have a significant impact on postfire land surface temperature change
- The sensitivity of land surface temperature change to fire regimes shows obvious latitudinal pattern

Supporting Information:

Supporting Information may be found in the online version of this article.

Correspondence to:

L. Wang and C. Yue,
wangliang.cn@163.com;
chaoyue@ms.iswc.ac.cn

Citation:

Zhao, J., Wang, L., Hou, X., Li, G., Tian, Q., Chan, E., et al. (2021). Fire regime impacts on postfire diurnal land surface temperature change over North American boreal forest. *Journal of Geophysical Research: Atmospheres*, *126*, e2021JD035589. https://doi.org/10.1029/2021JD035589

Received 13 OCT 2021

Abstract Wildfire is the most prevalent natural disturbance in the North American boreal forest (NABF) and can cause postfire land surface temperature change (ΔT_{fire}) through biophysical processes. Fire regimes, such as fire severity, fire intensity, and percentage of burned area (PBA), may influence ΔT_{fire} through their impacts on postfire vegetation damage and, if so, there may be important feedbacks between fire regime and climate warming through biophysical effects. Here, we employ satellite observations to investigate postfire diurnal ΔT_{fire} across NABF. We further use a stepwise multiple linear regression model to examine the driving factors for ΔT_{fire} by incorporating latitude, fire regime variables, and their interactions. Our results demonstrate a pronounced asymmetry in diurnal ΔT_{fire}, characterized by daytime warming in contrast to nighttime cooling. Clear latitudinal patterns are found in ΔT_{fire}, with stronger effects in lower latitudes. Such latitudinal patterns of ΔT_{fire}, especially the daytime one, are driven by both latitudinal patterns in fire regimes and an increased sensitivity of ΔT_{fire} to fire regime as the latitude decreases. The multiple linear regression model explains 37% of the variance in daytime ΔT_{fire}, whereas for the nighttime ΔT_{fire} the explanatory power is rather low (5%). For daytime ΔT_{fire}, fire severity accounted for most (43.65%) of the model explanatory power, followed by PBA (24.60%) and fire intensity (13.10%). Our results highlight important fire regime impacts on daytime ΔT_{fire} and, further, on the annual ΔT_{fire}, suggesting that fire might amplify future boreal climate change through positive feedbacks between fire regime and postfire surface warming.

1. Introduction

Boreal forests are the world's largest terrestrial biome and contains ~30% of the world's total forest cover (Veraverbeke et al., 2017). It stores about 35% of global soil organic carbon (Scharlemann et al., 2014) and 16% of global forest biomass carbon (Pan, Birdsey, et al., 2011). North American boreal forest (NABF) dynamics, carbon cycling (Balshi, McGuire, Duffy, Flannigan, Kicklighter, et al., 2009), and surface energy exchange (Amiro, Orchansky, et al., 2006; Randerson et al., 2006) are primarily driven by wildfire. In this region, the forests consist primarily of flammable evergreen conifers, including black spruce (*Picea mariana*), jack pine (*Pinus banksiana*), white spruce (*Picea glauca*), and to some extent in Eastern Canada, balsam fir (*Abies balsamea*), and white cedar (*Thuja occidentalis*) (Rogers et al., 2013). These species favor high-intensity crown fires that usually have a larger patch size and release more energy than their counterparts in boreal Eurasia (de Groot, Cantin, et al., 2013; Wooster, 2004). Fires in NABF typically kill most of the overstory trees, trigger a century-long vegetation succession, and have significant impacts on land surface temperature (LST) and the surface energy balance (Amiro, Barr, et al., 2006; Liu & Randerson, 2008; Randerson et al., 2006; Rogers et al., 2013). The relatively homogeneous fire behavior over NABF provides an excellent opportunity to examine fire effects on LST change.

Previous studies converge to demonstrate that immediately following fire, the change in LST is dominated by warming, largely due to a decrease in summer albedo, because of surface darkening, and reduced evaporative cooling caused by postfire vegetation damage (Liu et al., 2018). However, most of these studies investigated the change of mean daily LST (Rogers et al., 2013, 2015), and paid much less attention to diurnal LST changes. Nonetheless, a few studies have pointed out that a diurnal asymmetry exists in the postfire LST change (Liu

et al., 2018, 2019). For example, Liu et al. (2018) reported that Siberian boreal forest fires significantly increased the diurnal temperature range in LST (defined as the difference between daily maximum and minimum temperature). Liu et al. (2019) further investigated the spatial heterogeneity of global forest fire effects on daytime and nighttime LST (i.e., T_{max} and T_{min}). Again, they found that fire-induced forest loss caused daytime warming but a nighttime cooling effect in northern high latitudes (Liu et al., 2019). Despite this progress, there remains little information on how fire regime might influence the LST change by affecting vegetation damage and related biophysical processes.

Fire regime is a central concept describing fire behavior and its consequences on vegetation, including traits of burned area, fire season, fire intensity, fire severity, and fire size. Many studies have used this term, although the metrics employed are rather varied (Archibald et al., 2013; Beck et al., 2011; Bergeron et al., 2004; Chuvieco et al., 2008; de Groot, Cantin, et al., 2013; Heyerdahl et al., 2001; Kasischke & Turetsky, 2006; Kasischke et al., 2010). Here, we focus on three aspects of the NABF fire regime: fire severity, fire intensity, and percentage of burned area (PBA), which fundamentally drive NABF dynamics and their feedbacks to climate (Weber & Flannigan, 1997). Fire severity refers to the loss of organic matter or vegetation damage that occurs as the direct consequence of a fire, which is estimated here from remotely sensed vegetation index (Boby et al., 2010; Keeley, 2009). Fire intensity is measured as the energy released during active fire burning (Keeley, 2009). PBA reflects the spatial extent of burning and is defined as the percentage of burned area for a given region. In NABF, PBA drives fundamental regional forest dynamics, because fire is the dominant disturbance agent and affects both postfire forest species composition and regional forest age structure (Beck et al., 2011; Pan, Chen, et al., 2011). By affecting tree mortality and postfire organic layer thickness, both fire severity and fire intensity exert control over the immediate postfire vegetation damage, soil properties and the long-term vegetation successional trajectory (Beck et al., 2011; Harden et al., 2006). Previous studies found that more severe fires lead to increased levels of organic layer combustion, but promote the recruitment of deciduous broadleaf trees following fire (Beck et al., 2011; Johnstone & Kasischke, 2005; Johnstone et al., 2010). The decades-long persistence of broadleaf tree species during postfire forest succession can lead to elevated albedo and evapotranspiration and therefore a strong biophysical feedback on climate (Liu & Randerson, 2008; McMillan & Goulden, 2008).

Over the last 40 years, fire regimes in NABF have changed dramatically. Statistical data from national and state forestry agencies show a long-term increasing trend in burned area in Alaska (Kasischke & Turetsky, 2006; Kasischke et al., 2010) and Canada (Podur et al., 2002; Stocks et al., 2002). Turetsky et al. (2010) found that changes in fire regime characteristics, including increased total burned area and fire size and more frequent late-season burning, all positively affected the severity of surface fuel combustion, increasing boreal-fire carbon losses beyond the effects of changes in burned area alone (Turetsky et al., 2010). Fire regimes are expected to change further with the anticipated climate warming. Wotton et al. (2017) suggests that the challenges of wildfire management in Canada in the 21st century include not only dealing with the increasing number of fires, but also the increasing number of uncontrollable, high-intensity crown fires (Wotton et al., 2017). Indeed, studies using fire weather indices or climate models generally predict significant increases in the fire frequency and burned area across NABF by the end of the century (Balshi, McGuire, Duffy, Flannigan, Walsh, et al., 2009; Flannigan et al., 2005; Hu et al., 2010; Kasischke et al., 2010; Young et al., 2017). Such ongoing and anticipated changes in fire regime should influence the role of fire in regional climate regulation (Liu et al., 2019). However, to the best of our knowledge, no studies have quantified fire regime effects on postfire LST change or its diurnal patterns in the NABF.

Here, we use multiple satellite observations to investigate how fire regimes have influenced fire-induced daytime and nighttime LST change (ΔT_{fire}, i.e., the fire-induced difference between the LST one year after fire and that one year before fire) over the NABF. We further examine the latitudinal patterns in ΔT_{fire} and determine how such patterns are driven by fire regimes. We aim to address the following questions: (a) How do forest fires impact the diurnal LST change and what is the relative importance of the different biophysical processes controlling daytime ΔT_{fire}? (b) Do fire regimes affect ΔT_{fire} and, if so, what are the relative contributions of different fire regimes?

Table 1
Summary of the Moderate Resolution Imaging Spectroradiometer (MODIS) Data Products Used

Variable	Product name	Platform	Spatial resolution	Temporal resolution	Period
BA[a]	MCD64A1	Terra & Aqua	500 m	Monthly	2004–2017
LST[a]	MYD11C3	Aqua	0.05°	Monthly	2003–2018
FRP[a]	MCD14 ML	Terra & Aqua	1 km	Monthly	2004–2017
NDVI[a]	MYD13C2	Aqua	0.05°	Monthly	2003–2018
LCT[a]	MCD12C1	Terra & Aqua	0.05°	Yearly	2003–2016
ET[a]	MOD16A2	Terra	500 m	8 day	2003–2018
Albedo	MCD43C3	Terra & Aqua	0.05°	16 day	2003–2018

[a]BA = burned area, LST = land surface temperature, FRP = fire radiative power, NDVI = normalized difference vegetation index, LCT = land cover type, ET = evapotranspiration.

2. Data and Methods

2.1. Data Sets

We used 7 satellite-data products derived from the Moderate Resolution Imaging Spectroradiometer (MODIS). This MODIS-Collection consisted of products for burned area (BA), LST, fire radiative power (FRP), normalized difference vegetation index (NDVI), land cover type (LCT), evapotranspiration (ET), and albedo (α) at various resolutions (Table 1). Monthly gridded incoming shortwave solar radiation (SR) data at a 1° spatial resolution were used to calculate changes in net surface radiation due to postfire albedo change. Full details of these data sets, including quality control, data preparation, and other auxiliary information, can be found in the Supporting Information S1. The original data characteristics are summarized in Table 1.

2.2. Methodology

2.2.1. Fire-Induced Changes in LST, Albedo, NDVI, and Evapotranspiration

We employed a space-and-time approach to assess the fire-induced LST change at 0.05° resolution from 2004 to 2017, which can disentangle the effect of fire on LST from the background climate variation over time (Alkama & Cescatti, 2016).

The space-and-time methodology is based on Equation 1

$$\Delta T = \Delta T_{\text{fire}} + \Delta T_{\text{res}}, \tag{1}$$

which assumes that, for a given burned pixel, the gross change in LST between the years after and before fire (ΔT) is the sum of the LST change induced by fire (ΔT_{fire}) and a residual change caused by the interannual climate variability (ΔT_{res}) driven by factors other than fire, for example, by changes in large-scale circulation patterns.

Therefore, it follows that

$$\Delta T_{\text{fire}} = \Delta T - \Delta T_{\text{res}}. \tag{2}$$

In Equation 2, ΔT is readily obtained and ΔT_{res} can be approximated as the mean ΔT of the adjacent control pixels.

Here, for a given burned pixel, we overlaid a 10 × 10 pixel search window (longitude × latitude, approximately equal to 50 × 50 km) centering this burned pixel. Only unburned pixels within the search window with the same forest type as the given burned pixel were selected as adjacent control pixels. To test the robustness of this approach, we made a probability density plot of ΔT, ΔT_{res}, and ΔT_{fire} for the period 2004–2017 (Figure S1). The results show that the range of ΔT_{fire} was remarkably reduced compared with those of ΔT and ΔT_{res}, suggesting that the space-and-time approach is effective in removing background climate variation noise from the gross LST change and isolating the fire effect. In addition, we verified that no clear relationship existed between ΔT_{fire} and ΔT_{res}, given that neither daytime ΔT_{fire} or nighttime ΔT_{fire} is significantly correlated with ΔT_{res}. This likely

excludes potential interaction between ΔT_{fire} and ΔT_{res}, supporting that they could be separated using the "time-and-space" approach. Positive values of ΔT_{fire} indicate that forest fire had a warming effect, while negative values indicate cooling. For the sake of consistency, fire effects on albedo ($\Delta\alpha$), ET (ΔET), and NDVI (ΔNDVI) were calculated using a similar approach.

We have no special treatment for multiple times of burned pixels, because we verified that 98.02% of the burned pixels had only burned once during the entire study period. In addition, we verified that the ΔT_{res} is largely independently of the differences in NDVI and ET between the adjacent control pixel and the central burned pixel. Previous studies have found that forest albedo is mainly affected by forest type and NDVI, and the land surface temperature is mainly affected by albedo and ET (Bonan, 2015; Liu et al., 2018). So, the differences in NDVI, LST, ET, and albedo between the adjacent control pixel and the central burned pixel will not have a significant impact on ΔT_{res}. Therefore, we only selected the constraint condition of the same forest type to ensure the homogeneity of the central burned pixel and the adjacent control pixels in our space-and-time approach.

2.2.2. Changes in Surface Energy Fluxes Driven by Albedo and Evapotranspiration Changes

The major biophysical controls on ΔT_{max} include changes in absorbed incoming shortwave solar radiation (ΔSR) and latent heat flux (ΔLE). The former is caused by fire-induced surface albedo change ($\Delta\alpha$), while the latter is caused by fire-induced changes in evapotranspiration (ΔET). We quantified the relative contributions of albedo and ET changes to daytime ΔT_{fire} by converting both into energy fluxes. First, the contribution of albedo change is calculated as follows:

$$\Delta \mathrm{SR}_y = (1-\alpha_{y+1})\mathrm{SW}_{y+1} - (1-\alpha_{y-1})\mathrm{SW}_{y-1}, \tag{3}$$

where SW is incoming shortwave solar radiation, α is albedo, and y is the year of forest fire occurrence. The latent heat flux (LE, W m^{-2}) can be derived from the flux of evapotranspiration (E, mm day^{-1}) as follows:

$$\mathrm{LE} = \rho \mathrm{Lv} E, \tag{4}$$

where ρ is the density of water (1 kg m^{-3}) and Lv is the latent heat of vaporization of water (we used a constant value of 2.5×10^6 J kg^{-1}). From Equation 4, we can easily obtain the conversion coefficient between ET (mm day^{-1}) and LE as 28.94 W m^{-2}/(mm day^{-1}). Therefore, the change in latent heat flux (ΔLE) can be calculated as

$$\Delta \mathrm{LE} = \Delta \mathrm{ET} \times 28.94 \ \ \mathrm{W} \ \ \mathrm{m}^{-2}/(\mathrm{mm} \ \ \mathrm{day}^{-1}). \tag{5}$$

Although this method does not account for all the terms of the full surface energy budget, it does allow us to make direct comparisons in their relative importance between the two major biophysical processes (i.e., surface albedo and evapotranspiration), which have been shown to strongly driven postfire LST change in previous studies (Liu et al., 2018). In addition, there are great uncertainties in calculating the remaining energy flux terms (i.e., ground heat flux, net longwave radiation, or sensible heat flux), because too many parameters are required to calculate these energy terms and the available products on these fluxes cannot be reliably applied in our research due to their coarse spatial resolution, such as HIRS data on 1° resolution (Bonan, 2015; Gruber et al., 2007; Jung et al., 2019).

2.2.3. Quantifying Fire Regime Impacts on Postfire LST Change

Here, we focus on the effects of three fire regime variables on postfire LST change at a 0.05° spatial resolution. Fire intensity, fire severity, and PBA were expressed in terms of fire radiative power (FRP), the fire-induced NDVI change ($\Delta\mathrm{NDVI}_{fire}$), and the percentage of burned area, respectively. Detailed descriptions of the calculation of these three fire regime variables can be found in the Supporting Information S1.

We assessed the effects of fire regime variables on diurnal ΔT_{fire} using two linear regression methods. This analysis was limited to grid cells with a PBA greater than 0.2, to avoid the stochastic noise caused by too small a burned area. We first used bivariate simple linear regression to investigate the individual effects of each fire regime variable on diurnal ΔT_{fire}. The significance of the linear relationship was tested using the Student-t test with a confidence level of $p < 0.05$. To explore how the sensitivity of ΔT_{fire} to fire regime changes with latitude, we divided NABF into 10 2° latitude bands ranging from 46°N to 66°N. For each band, the sensitivity of ΔT_{fire} to fire regime was defined as the slope of the simple bivariate regression between ΔT_{fire} and the fire regime variables.

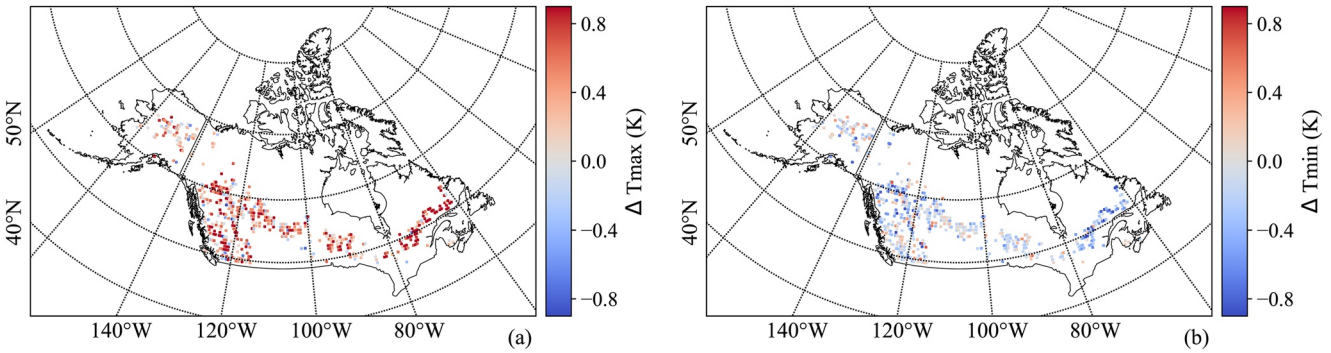

Figure 1. Changes in mean daily maximum and minimum land surface temperature (LST) one year after forest fire (ΔT_{max} and ΔT_{min}): (a) ΔT_{max}, (b) ΔT_{min}. T_{max} and T_{min} are approximated by LST retrieved at 13:30 and 01:30 local time, respectively, by the MODIS sensor onboard the Aqua satellite. Original analysis was made at 0.05° resolution but results are aggregated to 0.5° in this figure for display purposes.

We further used multiple linear regression in a stepwise manner to explore the relationship between ΔT_{fire} and several potential explanatory variables: $\Delta NDVI_{fire}$, LgFRP, PBA, latitude (Lat), and three interaction terms ($\Delta NDVI_{fire}$: Lat, LgFRP:Lat, and PBA:Lat, with the colon indicating the interaction term). We used the Forward and Backward stepwise elimination method in the MASS package in R to obtain an optimal model that yielded the lowest Akaike Information Criterion (AIC) value. Type II analysis of variance (Type II ANOVA) was used to examine the significance of the different terms included in the final linear regression model. This method respects the principle of marginality and examines the "partial" effect of each explanatory term by calculating the incremental F-statistic that contrasts the full model with an alternative model, in which the explanatory term in question is removed. We used the "LMG" method from the "relaimpo" R package to quantify the relative contributions of different explanatory terms to the total variance explained by the regression model.

3. Results

3.1. Postfire Daytime and Nighttime Land Surface Temperature Change

In most of the NABF, forest fires produced a marked increase of daily T_{max} (mean ΔT_{max} = 0.70 ± 0.71 K), and an overall small decrease in T_{min} one year after fire (mean ΔT_{min} = −0.21 ± 0.44 K) (Figures 1 and 2). The LST response to fire also exhibits pronounced seasonal patterns (Figure 2). The surface daytime warming effect, i.e., the increase in T_{max}, is greatest in summer (1.36 ± 1.02 K), followed by spring (0.57 ± 0.81 K) and autumn (0.25 ± 0.77 K), while a daytime cooling effect occurred in winter (−0.29 ± 0.82 K) (Figures 2 and S2). In contrast, changes in T_{min} following fire show consistent cooling effects for all four seasons, with only small variations (Figure 2). The cooling effect on T_{min} is largest in winter (−0.37 K ± 0.74 K), followed by spring (−0.28 ± 0.58 K) and summer (−0.26 ± 0.51 K), and smallest in autumn (−0.20 ± 0.58 K).

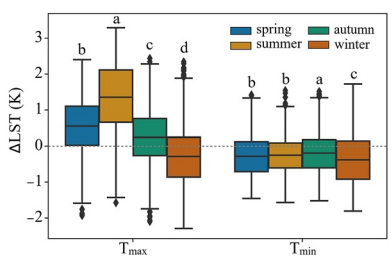

Figure 2. The effects of forest fire on the mean annual daily maximum and minimum land surface temperature (LST; ΔT_{fire}) in different seasons. The center line of the boxplot shows the median value, with box limits showing upper and lower quantiles and whiskers showing 1.5 × interquartile range and points showing outliers. The symbols a, b, c, and d represent significant differences ($p < 0.05$) among different seasons determined by analysis of variance (ANOVA).

The biophysical controls on ΔT_{max} included changes in latent heat flux caused by evapotranspiration (ET) and changes in absorbed shortwave radiation due to changes in surface albedo (α). Our results show that $\Delta\alpha$ and ΔET have distinct seasonal patterns and the dominant factors of ΔT_{max} are different in different seasons (Figures 3 and S3). One year after fire, the decrease in albedo during summer (−0.01 ± 0.01) is much less pronounced than the increase in winter (0.07 ± 0.06) (Figure 3a). In contrast, ET shows a clear reduction during summer (−15.47 ± 22.23 mm month^{-1}) while in winter it remains almost unchanged (−0.46 ± 1.24 mm month^{-1}) (Figure 3b).

If the effects of $\Delta\alpha$ and ΔET are expressed as energy fluxes to allow comparison, the strong decrease in summer latent heat flux (−4.97 ± 7.15 W m^{-2}) is almost three times the increase in absorbed shortwave radiation (SR) (1.55 ± 12.36 W m^{-2}) (Figures 3c and 3d), indicating that the increase in summer daytime LST is controlled more by the change in ET than by the change in albedo. In contrast, in winter, increased albedo following fire

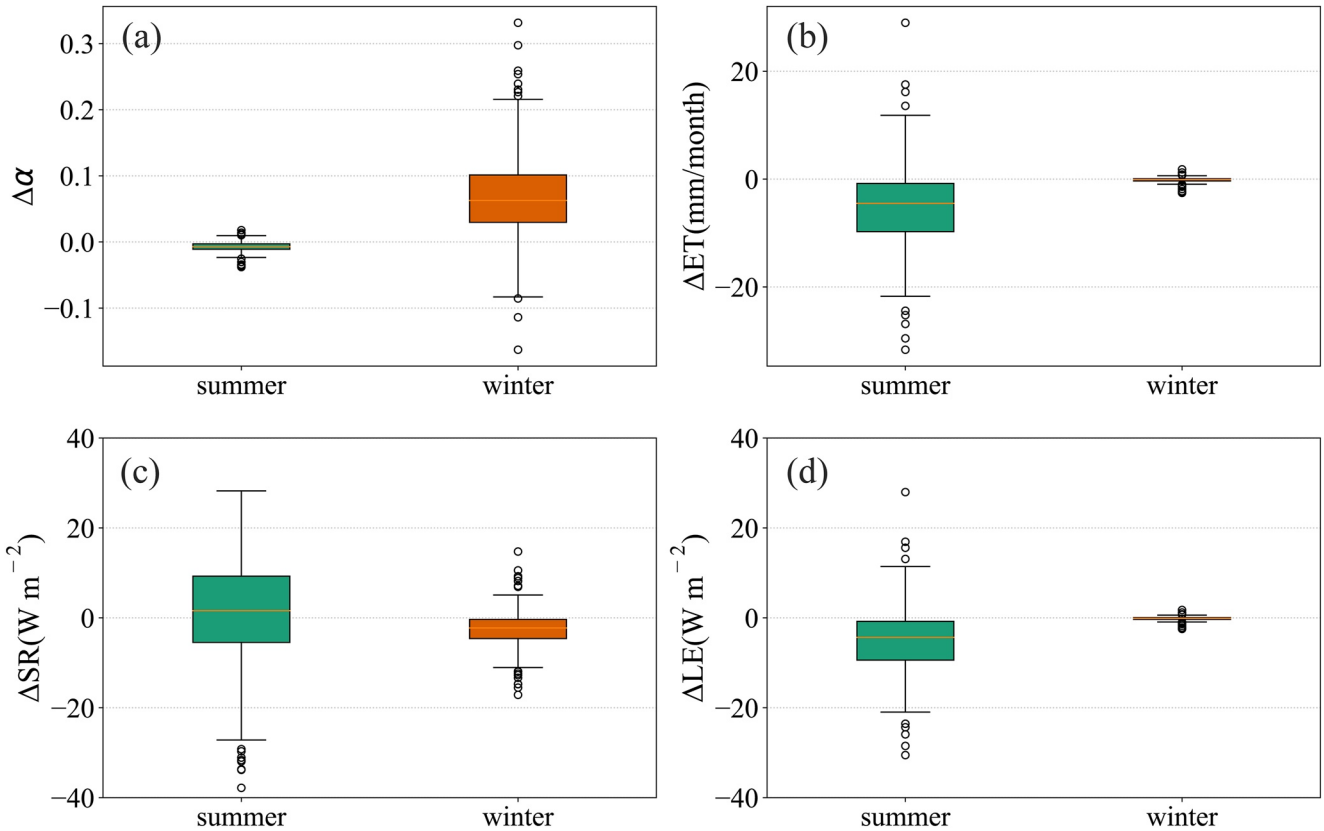

Figure 3. The effects of forest fire on albedo (a), evapotranspiration (ET) (b), absorbed net shortwave radiation (ΔSR) (c), and latent heat flux (ΔLE) (d) during summer and winter one year after fire. The center line of the boxplot shows the median value, with box limits showing upper and lower quartiles and whiskers showing 1.5 × interquartile range and points showing outliers.

results in a strong decrease in absorbed SR (-2.57 ± 3.83 W m^{-2}) while there is almost no change in the latent heat flux (-0.15 ± 0.40 W m^{-2}). This negligible change in latent heat flux in winter is unsurprising simply because vegetation is largely in dormancy with little physiological activity even without fire. Further, we found that the magnitude of increase of postfire winter albedo increases as the forest canopy height decreases, which reflects the greater effect of snow cover on shorter vegetation (Figure S4).

Fire effects on annual mean daytime and nighttime LST also exhibited clear latitudinal patterns (Figure 4a). The magnitudes of both ΔT_{max} and ΔT_{min} decrease with latitude, at rates of -0.08 and 0.01 K degree^{-1}, respectively. It is worth noting that at higher latitudes the fire effect on LST is almost neutral (Figure 4a). Latitudinal patterns are also found in fire regime variables and such patterns largely correspond with the patterns of postfire LST change (Figures 4b–4d), suggesting that variations in ΔT_{fire} could be closely linked to variations in fire regime. This possible relationship is examined in the next section.

3.2. Fire Regime Impacts on Postfire Land Surface Temperature Change

We first examined the relationships between fire-induced ΔT and the three fire regime variables using bivariate simple linear regression. All fire regime variables show significant correlation with both ΔT_{max} and ΔT_{min} (Figure 5). For T_{max}, a larger reduction in postfire NDVI leads to more elevated surface warming. Higher values of fire intensity and PBA are also associated with enhanced warming. This fact helps to explain that the decrease in FRP and ΔNDVI along an increasing latitude gradient, evident in Figure 4, likely drives the decrease in ΔT_{max} along the same latitude gradient. Figure 5 shows that the variance in ΔT_{max} is best explained by ΔNDVI ($R^2 = 0.30$), followed by PBA ($R^2 = 0.15$) and LgFRP ($R^2 = 0.09$), suggesting a likely greater influence of fire severity on ΔT_{max}. In comparison to ΔT_{max}, the relationships between ΔT_{min} and the fire regime variables are reversed, with consistently lower values of R^2.

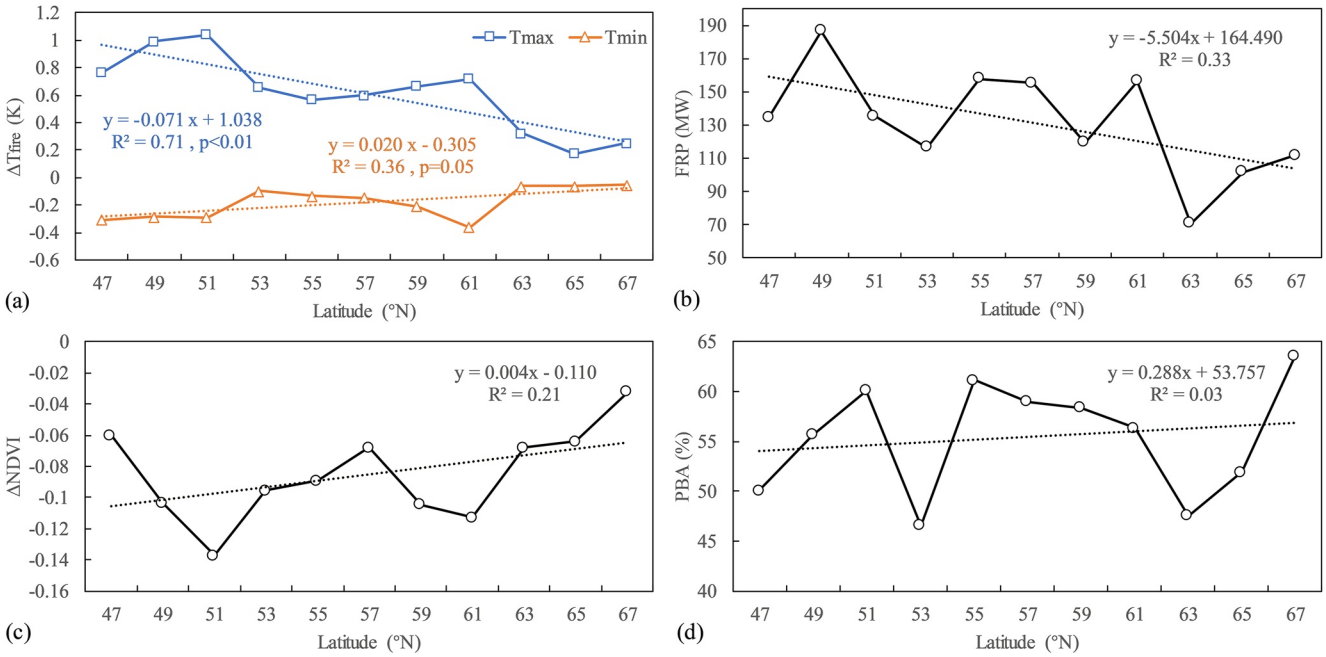

Figure 4. Latitudinal changes in diurnal ΔT_{fire} (a, T_{max}, and T_{min} for daytime and nighttime, respectively) after forest fires and latitudinal patterns of the three fire regime variables in North American boreal forest (NABF). (b) Fire radiative power; (c) fire-induced changes of normalized difference value index; (d) percentage of burned area. Dashed lines are linear regression lines.

The decrease in postfire ΔT_{fire} along an increasing latitude gradient shown in Figure 4 could be driven by the apparent changes in fire regimes, but it is possible that the sensitivity of ΔT_{fire} to fire regime variables (defined as the bivariate simple linear regression slope) also changes with latitude and provides an additional driver for latitudinal pattern of ΔT_{fire}. The investigation of this hypothesis is presented in Figure 6 which shows that the sensitivities of ΔT_{max} to both fire severity and PBA change significantly with latitude ($p < 0.05$). For example, the sensitivity of ΔT_{max} to ΔNDVI drops from −7.89°C per NDVI at 47°N to −2.08°C per NDVI at 65°N. In addition, the sensitivity of ΔT_{max} to FRP also decreases with latitude, albeit in an insignificant way. Similarly, the sensitivity of ΔT_{min} to all fire regimes also changes with latitude but these relationships are largely insignificant. These results suggest that fire regime not only affects postfire ΔT_{fire}, but also that such influences are strongly affected by interaction with latitude. Therefore, both latitudinal patterns of fire regimes and latitudinal patterns of sensitivities of ΔT_{fire} to fire regimes have contributed to the latitudinal patterns of ΔT_{fire}. These findings suggest significant impacts of fire regimes on postfire LST change.

It is clear that latitude, and the three fire regime variables, as well as the interactions between fire regime variables and latitude, are driving variations in postfire LST change. However, given that the three fire regime variables are significantly correlated with each other (Figure S5), it is impossible to discern the relative contributions of latitude and fire regime variables to the variations in ΔT_{fire} by using simple linear regressions. We therefore constructed a stepwise multiple linear regression model by incorporating ΔNDVI, LgFRP, PBA, and latitude, as well as the interactions between the three fire regime variables and latitude to quantify the relative contributions of different explanatory variables to ΔT_{fire} (Table 2 for ΔT_{max} and Table 3 for ΔT_{min}).

As shown in Table 2, ΔNDVI, LgFRP, PBA, and Lat, the interaction term between LgFRP and Lat (LgFRP:Lat), and the interaction term between PBA and Lat (PBA:Lat), collectively explain 37% of the variation in ΔT_{max}. Among the variables retained, ΔNDVI contributed the most (43.65%) to the explanatory power of the regression model, followed by PBA (24.60%), LgFRP (13.10%), Lat (7.37%), PBA:Lat (6.42%), and LgFRP:Lat (4.87%). The signs of the interaction terms of LgFRP:Lat and PBA:Lat are significantly negative, indicating that the sensitivity of ΔT_{max} to LgFRP and PBA decreases with latitude, consistent with the results shown in Figure 6. However, the explanatory power of the same variables for ΔT_{min} is rather small, explaining only 5% of its variation (Table 3). The explanatory variables retained are ΔNDVI and LgFRP, with relative importance values of 72.30% and 27.70%, respectively.

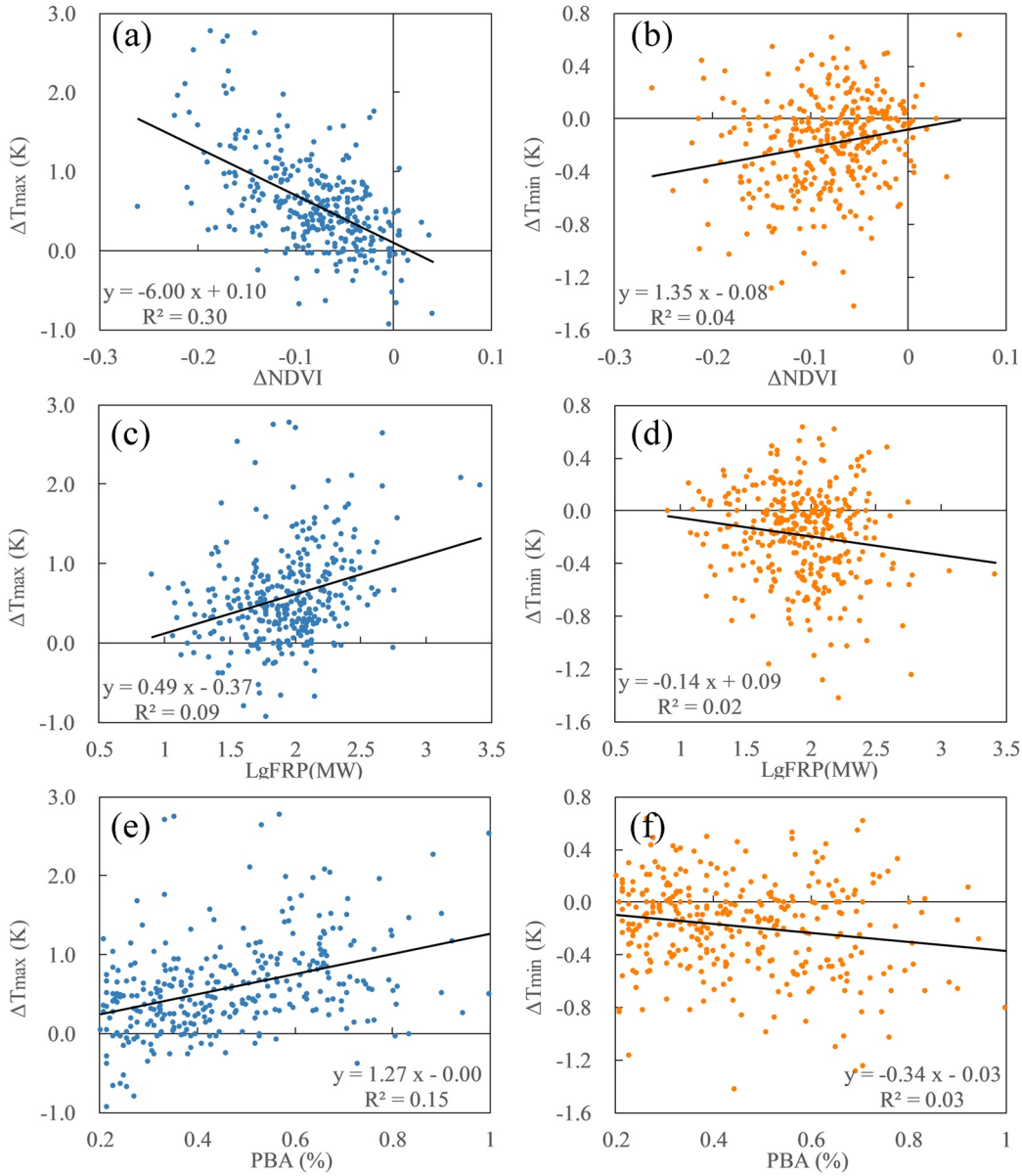

Figure 5. Bivariate regression relationships between fire-induced ΔT_{max} (a, c, e, n = 319), ΔT_{min} (b, d, f, n = 332) and the three fire regime variables: fire severity (measured by fire-induced ΔNDVI, a, b), fire intensity (measured by fire radiative power [FRP], c, d) and percentage of burned area (PBA) (e), (f). Solid dots represent mean values over 2 × 2° windows. Solid lines are linear regression lines, with all regressions being significant at a confidence level of 0.05.

4. Discussion

To date, satellite-data-based assessments of postfire LST change have adopted the space-for-time analogy, assuming that the LST difference between burned pixels and adjacent unburned pixels reflects the LST effect of fire over time (Liu et al., 2019). This approach is based on an implicit assumption that, prior to burning, the land surface temperatures of two adjacent pixels were comparable. The validity of this assumption has rarely been verified, however. Signals caused by differences in soil and vegetation properties between neighboring pixels, given the commonly large spatial distance used in previous studies (e.g., 50 × 28 km in Liu et al. (2019)), rather than by the fire effect, are expected to remain in the ΔT when it is calculated in this way. As an alternative approach, Rogers et al. (2013) simply calculated the fire effect as the temporal difference in LST for the years after and before fire, but ΔT derived by this approach is subject to the influence of large-scale background climate variations,

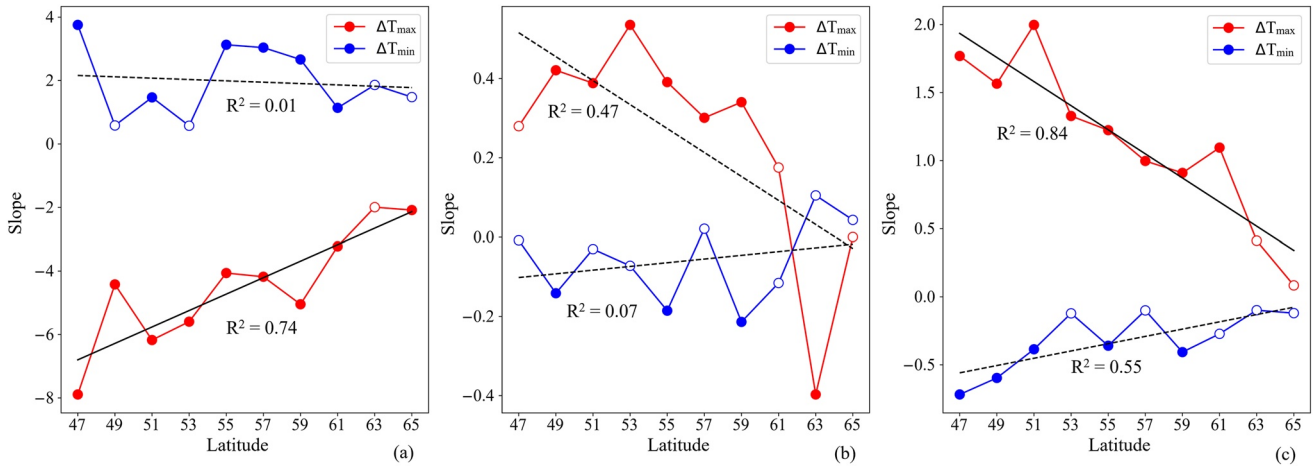

Figure 6. Changes in the regression slopes of ΔT against fire regimes (a, ΔNDVI; b, LgFRP; c, percentage of burned area [PBA]) along 2° moving windows. The horizontal axis indicates the center latitude of the 2° moving window. Solid (hollow) points indicate significant (insignificant) bivariate simple linear regressions between ΔT_{fire} and fire regime variable in each 2° latitude interval. Solid (dashed) lines represent significant (insignificant) linear regression lines between the slopes and latitude.

rather than only to the effects of fire. To overcome the limitations inherent in both approaches, we employed the space-and-time approach to assess the fire-induced LST change. This approach assumes that the ΔT_{res} values between two adjacent pixels are comparable, which is a much more conservative assumption that those used in the approaches of Liu et al. (2019) and Rogers et al. (2013). Results shown that our space-and-time method can effectively disentangle the effect of fire on LST from the background climate variation over time.

Land surface change due to various disturbances, such as forest fire, wind, and insect outbreaks, has been found to be an important feedback to future climate change (Brovkin et al., 2013). Although many studies have been carried out to examine the climate feedbacks due to forest fire (Randerson et al., 2006; Rogers et al., 2013), most of them have concentrated only on exploring the impact of fire on the average climate state (e.g., mean daily air temperature or mean daily LST). However, over the past few decades, global warming has shown clear diurnal asymmetry with the near-surface air temperature increasing faster during nighttime than daytime (Du et al., 2019; Easterling, 1997; Wen et al., 2018). In boreal North America, weather station observations show that the increasing rate of annual mean T_{min} over the past four decades is 1.67 and 2.14 times that of T_{max} in Canada and Alaska, respectively (Karl et al., 1993). However, the asymmetric effects of forest fire on diurnal ΔT have received less attention. Our results fill this gap and highlight the diurnal asymmetry in the magnitude and sign of the LST response to forest fires.

Table 2
Results of a Stepwise Multiple Linear Regression of Postfire ΔT_{max} Against Explanatory Variables

	Estimate	Standard error	Type II ANOVA		Relative importance (%)
			F-value	Pr(>*F*)	
ΔNDVI	−3.99	0.66	36.26	***	43.65
LgFRP	2.21	0.91	5.15	*	13.10
PBA	4.07	1.79	6.30	*	24.60
Lat	0.09	0.03	4.99	**	7.37
LgFRP:Lat	−0.04	0.02	4.98	*	4.87
PBA:Lat	−0.06	0.03	4.06	*	6.42

Note. Results of Type II ANOVA and the relative importance analysis are also shown. An *F*-test for the overall significance of the regression model yields a *p*-value < 0.01, with $R^2 = 0.37$. Pr(>*F*) is the probability of an *F*-value greater than the value given in the "*F*-value" column. Symbols for the significance test are: * for $p < 0.05$, ** for $p < 0.01$, and *** for $p < 0.001$.

In accordance with previous studies, our results indicate that boreal forest fires produce an annual warming effect one year after fire, which is mainly the result of strong summer daytime warming (Liu et al., 2018; Rogers et al., 2015). Rogers et al. (2015) proposed that reduced summer albedo caused by surface charring following fire might have increased LST during summertime, but they did not quantify the magnitude of albedo decline. Consequently, the relative importance of changes in albedo and evapotranspiration in driving postfire LST change has, so far, remained elusive. We found that the albedo decrease in summer only caused a slight increase in average summer net shortwave radiation (1.55 W ± 12.36 W m^{-2}) but LE decreased more sharply (−4.97 ± 7.15 W m^{-2}) one year after fire in NABF (Figure 3). Thus, the reduction of ET, rather than decreased albedo, is primarily responsible for observed postfire daytime warming. Liu et al. (2018) investigated postfire summer albedo change in boreal forest of eastern Siberia. They also reported a small albedo decline in summer (maximum decline of 0.02), similar to our finding of a mean decline of 0.01 in NABF. This agreement confirms the fact that, although the fire behaviors of boreal forests in North

Table 3
Results of a Stepwise Multiple Linear Regression of ΔT_{min} Against Explanatory Variables

	Estimate	Standard error	Type II ANOVA		Relative importance
			F-value	Pr(>*F*)	
ΔNDVI	1.17	0.36	10.39	**	72.30%
LgFRP	−0.09	0.05	2.48	0.12	27.70%

Note. Results of Type II ANOVA and the relative importance analysis are also shown. An *F*-test for the overall significance of the regression model yields a p-value < 0.01, with $R^2 = 0.05$. Pr(>*F*) is the probability of an *F*-value greater than the value given in the "*F*-value" column. Symbols for the significance test are: ** for $p < 0.01$.

America and Siberia are quite different (high-intensity canopy fires in North America versus low-intensity surface fires in Siberia) (Rogers et al., 2015), summer albedo changes following fire are surprisingly similar and small.

We found that postfire nighttime ΔT_{fire} is dominated by surface cooling in NABF. There are several possible explanations for this phenomenon. First, several studies examining deforestation effects on LST have shown that the removal of forest canopy can reduce roughness-generated turbulence, which could otherwise bring heat from the air aloft to the surface during night (Lee et al., 2011; Schultz et al., 2017). Removal of the forest canopy by fire would have a similar effect of reducing the coupling between the near-surface air and the land surface at night, contributing to postfire surface cooling. Second, forest fires in North America generally increased postfire albedo during fall, winter, and spring (Jin et al., 2012; Liu & Randerson, 2008; Wang et al., 2016). Daytime energy absorption is thus reduced compared to the prefire state. As a result, energy release during the night is also reduced and this indirectly contributes to nighttime cooling. Third, several field studies have shown that soil moisture decreases after fire in NABF (Harden et al., 2006; Holden et al., 2015), which further reduces soil heat capacity and daytime heat storage, and consequently nighttime heating (Dai et al., 1999; Peng et al., 2014).

Our results reveal that fire effects on T_{max} exhibit a distinct latitudinal pattern (Figure 4) as fires have a larger impact on daytime ΔT in lower latitudes than in higher ones. First, such a latitudinal pattern is primarily linked to latitudinal patterns of fire regimes. Stepwise multiple linear regression analysis indicates that latitude per se only contributes to 7.4% of the total explanatory power of the model, while fire regime variables collectively contribute to about 80% of the model explanatory power (Table 2). Second, even given a constant fire regime with latitude, the sensitivities of ΔT_{max} to fire intensity and burned area show significant dependence on latitude, with higher values in higher-latitude regions (Table 2). The interaction terms between fire regime and latitude explain >10% of the total model explanatory power. In summary, fire regimes have a significant impact on postfire daytime ΔT_{fire}.

Postfire ΔT_{min} follows a similar latitudinal pattern to ΔT_{max}, despite the fact that the explanatory power of the multiple linear regression model incorporating fire regime variables is much less than that for ΔT_{max} (5% versus 37%). However, this result echoes the findings of Schultz et al. (2017), who showed that the nighttime surface cooling effect following deforestation decreases from the midboreal region (~50°N) to the high-latitude region (~70°N). They found that the decrease in ΔT_{min} strongly correlates with the two dominant mechanisms explaining land surface cooling following forest removal: daytime heat storage and the strength of the nighttime surface-to-air temperature inversion. Therefore, the decrease in ΔT_{min} with increasing latitude may be first explained by the decrease in radiation with increasing latitude, i.e., lower-latitude regions have a greater decrease in absorbed energy during the daytime because of albedo decrease in spring, autumn, and winter. Second, as forest canopy height decreases with latitude (Figure S6), lower-latitude regions have stronger surface turbulence during the night if forest had not been impacted by fire, thus explaining the larger decrease in nighttime LST because of the greater loss of heat exchange from the air above the forest canopy.

We acknowledge that although the stepwise multiple linear regression of ΔLST (ΔT_{max} and ΔT_{min}) against explanatory variables all passed the significance test, the determination coefficients are rather low (37% and 5%). This suggests that other factors except for those considered in our model may influence ΔLST following forest fire. First, forest type may affect ΔT_{max} after forest fire, given that differences existed in canopy conductances, evapotranspiration, and albedo of in different forest types (Anderson et al., 2010; Breuer et al., 2003; Eugster

et al., 2000; Jackson et al., 2008). Second, fire size usually links to inevitable ecological consequences such as postfire vegetation damage (Adams, 2013; Cansler & McKenzie, 2014). Therefore, fire size may be an essential factor affecting the amplitude of ΔLST. Third, previous studies have shown that the decrease in surface albedo after afforestation is highly positively correlated with snow frequency (Li et al., 2015). Therefore, we suspect that the snow frequency and snow cover duration can exert strong influence over fire-induced albedo cooling effect. Although one can expect that snow duration should be highly correlated with latitude, which was already included in our model, variables of snow cover or snow depth were not explicitly included. In summary, the omission of above factors or processes in our analysis may contribute to low explanation power of our model for postfire ΔT_{max}.

Unfortunately, the model explanation power for postfire ΔT_{min} is even lower (5%). But we also note that various previous efforts trying to explain variations in ΔT_{min} following either afforestation or deforestation rarely succeeded. Heat storage change and temperature inversion strengths are the two major mechanisms used to explain ΔT_{min}. However, studies failed to identify large contributions by either of them. For instance, Li et al. (2015) found that postfire change in net shortwave radiation (i.e., a proxy for heat storage during daytime) explained only ~10% of the variations in ΔT_{min} following potential afforestation over the global scale. Schultz et al. (2017) performed details analysis regarding the role of heating potential and temperature inversion strength on nighttime ΔT following deforestation. They identified <20% of variations in ΔT_{min} could be explained by these two factors. In our study, we considered only fire regime variables and therefore, the 5% explanation power is something that's could be expected given the findings from these previous studies. The signal of ΔT_{min} itself is smaller than ΔT_{max}, increasing the difficulty for a complete explanation. But, in general, we acknowledge the shortcomings in our model (i.e., very limited explanation power) and the need for more thorough investigations on potential drivers for ΔT_{min}.

Our results highlight the fact that fire regimes have a significant positive influence on the daytime LST increase after fire, which ultimately drives the annual temperature increase. Strong climate-fire feedbacks may thus be expected in boreal North American ecosystems where forest fires are predicted to become more frequent and more severe in the future (de Groot, Flannigan, & Cantin, 2013; Grosse et al., 2011; Johnstone et al., 2010). If an intensified boreal fire regime unfolds as predicted, the magnitude of the initial positive climate effects following fire will be enhanced, with far-reaching influence on future climate change. Multiple lines of evidence, including increases in PBA, fire intensity, fire severity, fire emissions, and permafrost thaw, suggest that biogeochemical and biophysical processes are in rapid change in boreal forest ecosystems. Fire disturbance thus might play a catalytic role to speed up climate change by inducing positive feedback loops between fire intensity, fire severity, fire extent, and local land surface warming (Seidl et al., 2017).

5. Conclusion

Using multiple satellite observations, we examined the changes of daytime (ΔT_{max}) and nighttime (ΔT_{min}) land surface temperatures following fire in NABF and examined the role of fire regimes in driving such changes. Our results show that: (a) postfire LST change shows asymmetry between day and night. Forest fires cause surface warming during daytime but cooling at night. Postfire daytime warming primarily occurs in summer, whereas daytime surface cooling occurs in winter. Decreases in ET dominated daytime warming effects in summer, whereas increases in albedo contributed to daytime cooling in winter. (b) Both ΔT_{max} and ΔT_{min} exhibit clear latitudinal patterns, with strong effects occurring in lower-latitude regions, whereas in higher-latitude regions fire effects on LST are almost neutral. Such latitudinal patterns of LST change, especially ΔT_{max}, are found to be strongly driven by both latitudinal patterns in fire regimes and the increasing sensitivity of ΔT_{max} to fire regimes with increasing latitude. We therefore conclude that fire regime has an impact on postfire land surface temperature change in North American boreal forest, and the feedback between fire regime and land surface warming might accelerate climate and ecosystem changes in this region.

Conflict of Interest

The authors declare no conflicts of interest relevant to this study.

Data Availability Statement

The MODIS data were freely obtained from NASA's Earth Observing System Data and Information (https://ladsweb.modaps.eosdis.nasa.gov/).

Acknowledgments
This work was financially supported by the National Natural Science Foundation of China (U20A2090), the Strategic Priority Research Program of Chinese Academy of Sciences (XDB40000000) and the Open Research Foundation of Shandong Provincial Key Laboratory of Water and Soil Conservation and Environmental Protection of Linyi University (STKF201926).

References

Adams, M. A. (2013). Mega-fires, tipping points and ecosystem services: Managing forests and woodlands in an uncertain future. *Forest Ecology and Management*, *294*, 250–261. https://doi.org/10.1016/j.foreco.2012.11.039

Alkama, R., & Cescatti, A. (2016). Biophysical climate impacts of recent changes in global forest cover. *Science*, *351*, 600–604. https://doi.org/10.1126/science.aac8083

Amiro, B., Barr, A., Black, T., Iwashita, H., Kljun, N., Mccaughey, J., et al. (2006). Carbon, energy and water fluxes at mature and disturbed forest sites, Saskatchewan, Canada. *Agricultural and Forest Meteorology*, *136*, 237–251. https://doi.org/10.1016/j.agrformet.2004.11.012

Amiro, B. D., Orchansky, A. L., Barr, A. G., Black, T. A., Chambers, S. D., Chapin, F. S., III, et al. (2006). The effect of post-fire stand age on the boreal forest energy balance. *Agricultural and Forest Meteorology*, *140*, 41–50. https://doi.org/10.1016/j.agrformet.2006.02.014

Anderson, R. G., Canadell, J. G., Randerson, J. T., Jackson, R. B., Hungate, B. A., Baldocchi, D. D., et al. (2010). Biophysical considerations in forestry for climate protection. *Frontiers in Ecology and the Environment*, *9*, 174–182. https://doi.org/10.1890/090179

Archibald, S., Lehmann, C. E., Gomez-Dans, J. L., & Bradstock, R. A. (2013). Defining pyromes and global syndromes of fire regimes. *Proceedings of the National Academy of Sciences of the United States of America*, *110*, 6442–6447. https://doi.org/10.1073/pnas.1211466110

Balshi, M. S., McGuire, A. D., Duffy, P., Flannigan, M., Kicklighter, D. W., & Melillo, J. (2009). Vulnerability of carbon storage in North American boreal forests to wildfires during the 21st century. *Global Change Biology*, *15*, 1491–1510. https://doi.org/10.1111/j.1365-2486.2009.01877.x

Balshi, M. S., McGuire, A. D., Duffy, P., Flannigan, M., Walsh, J., & Melillo, J. (2009). Assessing the response of area burned to changing climate in western boreal North America using a Multivariate Adaptive Regression Splines (MARS) approach. *Global Change Biology*, *15*, 578–600. https://doi.org/10.1111/j.1365-2486.2008.01679.x

Beck, P. S. A., Goetz, S. J., Mack, M. C., Alexander, H. D., Jin, Y., Randerson, J. T., & Loranty, M. M. (2011). The impacts and implications of an intensifying fire regime on Alaskan boreal forest composition and albedo. *Global Change Biology*, *17*, 2853–2866. https://doi.org/10.1111/j.1365-2486.2011.02412.x

Bergeron, Y., Gauthier, S., Flannigan, M., & Kafka, V. (2004). Fire regimes at the transition between mixed wood and coniferous boreal forest in Northwestern Quebec. *Ecology*, *85*, 1916–1932. https://doi.org/10.1890/02-0716

Boby, L. A., Schuur, E. A. G., Mack, M. C., Verbyla, D., & Johnstone, J. F. (2010). Quantifying fire severity, carbon, and nitrogen emissions in Alaska's boreal forest. *Ecological Applications*, *20*, 1633–1647. https://doi.org/10.1890/08-2295.1

Bonan, G. (2015). *Ecological climatology: Concepts and applications*. Cambridge, UK: Cambridge University Press.

Breuer, L., Eckhardt, K., & Frede, H.-G. (2003). Plant parameter values for models in temperate climates. *Ecological Modelling*, *169*, 237–293. https://doi.org/10.1016/s0304-3800(03)00274-6

Brovkin, V., Boysen, L., Arora, V. K., Boisier, J. P., Cadule, P., Chini, L., et al. (2013). Effect of anthropogenic land-use and land-cover changes on climate and land carbon storage in CMIP5 projections for the twenty-first century. *Journal of Climate*, *26*, 6859–6881. https://doi.org/10.1175/jcli-d-12-00623.1

Cansler, C. A., & McKenzie, D. (2014). Climate, fire size, and biophysical setting control fire severity and spatial pattern in the northern Cascade Range, USA. *Ecological Applications*, *24*, 1037–1056. https://doi.org/10.1890/13-1077.1

Chuvieco, E., Giglio, L., & Justice, C. (2008). Global characterization of fire activity: Toward defining fire regimes from Earth observation data. *Global Change Biology*, *14*, 1488–1502. https://doi.org/10.1111/j.1365-2486.2008.01585.x

Dai, A., Trenberth, K. E., & Karl, T. R. (1999). Effects of clouds, soil moisture, precipitation, and water vapor on diurnal temperature range. *Journal of Climate*, *12*, 2451–2473. https://doi.org/10.1175/1520-0442(1999)012<2451:eocsmp>2.0.co;2

de Groot, W. J., Cantin, A. S., Flannigan, M. D., Soja, A. J., Gowman, L. M., & Newbery, A. (2013). A comparison of Canadian and Russian boreal forest fire regimes. *Forest Ecology and Management*, *294*, 23–34.

de Groot, W. J., Flannigan, M. D., & Cantin, A. S. (2013). Climate change impacts on future boreal fire regimes. *Forest Ecology and Management*, *294*, 35–44.

Du, Z., Zhao, J., Liu, X., Wu, Z., & Zhang, H. (2019). Recent asymmetric warming trends of daytime versus nighttime and their linkages with vegetation greenness in temperate China. *Environmental Science and Pollution Research*, *26*, 35717–35727. https://doi.org/10.1007/s11356-019-06440-z

Easterling, D. R., Horton, B., Jones, P. D., Peterson, T. C., Karl, T. R., Parker, D. E., et al. (1997). Maximum and minimum temperature trends for the globe. *Science*, *277*, 364–367. https://doi.org/10.1126/science.277.5324.364

Eugster, W., Rouse, W. R., Pielke, Sr, R. A., Mcfadden, J. P., Baldocchi, D. D., Kittel, T. G. F., et al. (2000). Land-atmosphere energy exchange in Arctic tundra and boreal forest: Available data and feedbacks to climate. *Global Change Biology*, *6*, 84–115. https://doi.org/10.1046/j.1365-2486.2000.06015.x

Flannigan, M. D., Logan, K. A., Amiro, B. D., Skinner, W. R., & Stocks, B. J. (2005). Future area burned in Canada. *Climatic Change*, *72*, 1–16. https://doi.org/10.1007/s10584-005-5935-y

Grosse, G., Harden, J., Turetsky, M., McGuire, A. D., Camill, P., Tarnocai, C., et al. (2011). Vulnerability of high-latitude soil organic carbon in North America to disturbance. *Journal of Geophysical Research*, *116*, G00K06. https://doi.org/10.1029/2010JG001507

Gruber, A., Lee, H.-T., Ellingson, R. G., & Laszlo, I. (2007). Development of the HIRS outgoing longwave radiation climate dataset. *Journal of Atmospheric and Oceanic Technology*, *24*, 2029–2047.

Harden, J. W., Manies, K. L., Turetsky, M. R., & Neff, J. C. (2006). Effects of wildfire and permafrost on soil organic matter and soil climate in interior Alaska. *Global Change Biology*, *12*, 2391–2403. https://doi.org/10.1111/j.1365-2486.2006.01255.x

Heyerdahl, E. K., Brubaker, L. B., & Agee, J. K. (2001). Spatial controls of historical fire regimes: A multiscale example from the interior west, USA. *Ecology*, *82*, 660–678. https://doi.org/10.1890/0012-9658(2001)082[0660:scohfr]2.0.co;2

Holden, S. R., Berhe, A. A., & Treseder, K. K. (2015). Decreases in soil moisture and organic matter quality suppress microbial decomposition following a boreal forest fire. *Soil Biology and Biochemistry*, *87*, 1–9. https://doi.org/10.1016/j.soilbio.2015.04.005

Hu, F. S., Higuera, P. E., Walsh, J. E., Chapman, W. L., Duffy, P. A., Brubaker, L. B., & Chipman, M. L. (2010). Tundra burning in Alaska: Linkages to climatic change and sea ice retreat. *Journal of Geophysical Research*, *115*, G04002. https://doi.org/10.1029/2009JG001270

Jackson, R. B., Randerson, J. T., Canadell, J. G., Anderson, R. G., Avissar, R., Baldocchi, D. D., et al. (2008). Protecting climate with forests. *Environmental Research Letters*, *3*, 044006.
Jin, Y., Randerson, J. T., Goulden, M. L., & Goetz, S. J. (2012). Post-fire changes in net shortwave radiation along a latitudinal gradient in boreal North America. *Geophysical Research Letters*, *39*, L13403. https://doi.org/10.1029/2012GL051790
Johnstone, J. F., Hollingsworth, T. N., Chapin, F. S., & Mack, M. C. (2010). Changes in fire regime break the legacy lock on successional trajectories in Alaskan boreal forest. *Global Change Biology*, *16*, 1281–1295. https://doi.org/10.1111/j.1365-2486.2009.02051.x
Johnstone, J. F., & Kasischke, E. S. (2005). Stand-level effects of soil burn severity on postfire regeneration in a recently burned black spruce forest. *Canadian Journal of Forest Research*, *35*, 2151–2163. https://doi.org/10.1139/x05-087
Jung, M., Koirala, S., Weber, U., Ichii, K., Gans, F., Camps-Valls, G., et al. (2019). The FLUXCOM ensemble of global land-atmosphere energy fluxes. *Scientific Data*, *6*, 74. https://doi.org/10.1038/s41597-019-0076-8
Karl, T. R., Knight, R. W., Gallo, K. P., Peterson, T. C., Jones, P. D., Kukla, G., et al. (1993). A new perspective on recent global warming: Asymmetric trends of daily maximum and minimum temperature. *Bulletin of the American Meteorological Society*, *74*, 1007–1023. https://doi.org/10.1175/1520-0477(1993)074<1007:anporg>2.0.co;2
Kasischke, E. S., & Turetsky, M. R. (2006). Recent changes in the fire regime across the North American boreal region—Spatial and temporal patterns of burning across Canada and Alaska. *Geophysical Research Letters*, *33*, L09703. https://doi.org/10.1029/2006GL025677
Kasischke, E. S., Verbyla, D. L., Rupp, T. S., McGuire, A. D., Murphy, K. A., Jandt, R., et al. (2010). Alaska's changing fire regime—Implications for the vulnerability of its boreal forests. *Canadian Journal of Forest Research*, *40*, 1313–1324. https://doi.org/10.1139/x10-098
Keeley, J. E. (2009). Fire intensity, fire severity and burn severity: A brief review and suggested usage. *International Journal of Wildland Fire*, *18*, 116–126. https://doi.org/10.1071/wf07049
Lee, X., Goulden, M. L., Hollinger, D. Y., Barr, A., Black, T. A., Bohrer, G., et al. (2011). Observed increase in local cooling effect of deforestation at higher latitudes. *Nature*, *479*, 384–387. https://doi.org/10.1038/nature10588
Li, Y., Zhao, M., Motesharrei, S., Mu, Q., Kalnay, E., & Li, S. (2015). Local cooling and warming effects of forests based on satellite observations. *Nature Communications*, *6*, 6603. https://doi.org/10.1038/ncomms7603
Liu, H., & Randerson, J. T. (2008). Interannual variability of surface energy exchange depends on stand age in a boreal forest fire chronosequence. *Journal of Geophysical Research*, *113*, G01006. https://doi.org/10.1029/2007JG000483
Liu, Z., Ballantyne, A. P., & Cooper, L. A. (2018). Increases in land surface temperature in response to fire in Siberian boreal forests and their attribution to biophysical processes. *Geophysical Research Letters*, *45*, 6485–6494. https://doi.org/10.1029/2018GL078283
Liu, Z., Ballantyne, A. P., & Cooper, L. A. (2019). Biophysical feedback of global forest fires on surface temperature. *Nature Communications*, *10*, 214. https://doi.org/10.1038/s41467-018-08237-z
McMillan, A. M. S., & Goulden, M. L. (2008). Age-dependent variation in the biophysical properties of boreal forests. *Global Biogeochemical Cycles*, *22*, GB2019. https://doi.org/10.1029/2007GB003038
Pan, Y., Birdsey, R. A., Fang, J., Houghton, R., Kauppi, P. E., Kurz, W. A., et al. (2011). A large and persistent carbon sink in the world's forests. *Science*, *333*, 988–993. https://doi.org/10.1126/science.1201609
Pan, Y., Chen, J. M., Birdsey, R., McCullough, K., He, L., & Deng, F. (2011). Age structure and disturbance legacy of North American forests. *Biogeosciences*, *8*, 715–732. https://doi.org/10.5194/bg-8-715-2011
Peng, S. S., Piao, S., Zeng, Z., Ciais, P., Zhou, L., Li, L. Z. X., et al. (2014). Afforestation in China cools local land surface temperature. *Proceedings of the National Academy of Sciences of the United States of America*, *111*, 2915–2919. https://doi.org/10.1073/pnas.1315126111
Podur, J., Martell, D. L., & Knight, K. (2002). Statistical quality control analysis of forest fire activity in Canada. *Canadian Journal of Forest Research*, *32*, 195–205. https://doi.org/10.1139/x01-183
Randerson, J. T., Liu, H., Flanner, M. G., Chambers, S. D., Jin, Y., Hess, P. G., et al. (2006). The impact of boreal forest fire on climate warming. *Science*, *314*, 1130–1132. https://doi.org/10.1126/science.1132075
Rogers, B. M., Randerson, J. T., & Bonan, G. B. (2013). High-latitude cooling associated with landscape changes from North American boreal forest fires. *Biogeosciences*, *10*, 699–718. https://doi.org/10.5194/bg-10-699-2013
Rogers, B. M., Soja, A. J., Goulden, M. L., & Randerson, J. T. (2015). Influence of tree species on continental differences in boreal fires and climate feedbacks. *Nature Geoscience*, *8*, 228–234. https://doi.org/10.1038/ngeo2352
Scharlemann, J. P. W., Tanner, E. V. J., Hiederer, R., & Kapos, V. (2014). Global soil carbon: Understanding and managing the largest terrestrial carbon pool. *Carbon Management*, *5*, 81–91. https://doi.org/10.4155/cmt.13.77
Schultz, N. M., Lawrence, P. J., & Lee, X. (2017). Global satellite data highlights the diurnal asymmetry of the surface temperature response to deforestation. *Journal of Geophysical Research: Biogeosciences*, *122*, 903–917. https://doi.org/10.1002/2016JG003653
Seidl, R., Thom, D., Kautz, M., Martin-Benito, D., Peltoniemi, M., Vacchiano, G., et al. (2017). Forest disturbances under climate change. *Nature Climate Change*, *7*, 395–402. https://doi.org/10.1038/nclimate3303
Stocks, B. J., Mason, J. A., Todd, J. B., Bosch, E. M., Wotton, B. M., Amiro, B. D., et al. (2002). Large forest fires in Canada, 1959–1997. *Journal of Geophysical Research*, *108*(D1), 8149. https://doi.org/10.1029/2001JD000484
Turetsky, M. R., Kane, E. S., Harden, J. W., Ottmar, R. D., Manies, K. L., Hoy, E., & Kasischke, E. S. (2010). Recent acceleration of biomass burning and carbon losses in Alaskan forests and peatlands. *Nature Geoscience*, *4*, 27–31. https://doi.org/10.1038/ngeo1027
Veraverbeke, S., Rogers, B. M., Goulden, M. L., Jandt, R. R., Miller, C. E., Wiggins, E. B., & Randerson, J. T. (2017). Lightning as a major driver of recent large fire years in North American boreal forests. *Nature Climate Change*, *7*, 529–534. https://doi.org/10.1038/nclimate3329
Wang, Z., Erb, A. M., Schaaf, C. B., Sun, Q., Liu, Y., Yang, Y., et al. (2016). Early spring post-fire snow albedo dynamics in high latitude boreal forests using Landsat-8 OLI data. *Remote Sensing of Environment*, *185*, 71–83. https://doi.org/10.1016/j.rse.2016.02.059
Weber, M. G., & Flannigan, M. D. (1997). Canadian boreal forest ecosystem structure and function in a changing climate: Impact on fire regimes. *Environmental Reviews*, *5*, 145–166. https://doi.org/10.1139/a97-008
Wen, Y., Liu, X., Pei, F., Li, X., & Du, G. (2018). Non-uniform time-lag effects of terrestrial vegetation responses to asymmetric warming. *Agricultural and Forest Meteorology*, *252*, 130–143. https://doi.org/10.1016/j.agrformet.2018.01.016
Wooster, M. J. (2004). Boreal forest fires burn less intensely in Russia than in North America. *Geophysical Research Letters*, *31*, L20505. https://doi.org/10.1029/2004GL020805
Wotton, B. M., Flannigan, M. D., & Marshall, G. A. (2017). Potential climate change impacts on fire intensity and key wildfire suppression thresholds in Canada. *Environmental Research Letters*, *12*, 095003. https://doi.org/10.1088/1748-9326/aa7e6e
Young, A. M., Higuera, P. E., Duffy, P. A., & Hu, F. S. (2017). Climatic thresholds shape northern high-latitude fire regimes and imply vulnerability to future climate change. *Ecography*, *40*, 606–617. https://doi.org/10.1111/ecog.02205

References From the Supporting Information

Barrett, K., & Kasischke, E. S. (2013). Controls on variations in MODIS fire radiative power in Alaskan boreal forests: Implications for fire severity conditions. *Remote Sensing of Environment*, *130*, 171–181.

Chafer, C. J., Noonan, M., & Macnaught, E. (2004). The post-fire measurement of fire severity and intensity in the Christmas 2001 Sydney wildfires. *International Journal of Wildland Fire*, *13*(2), 227–241.

Díaz-Delgado, R., Lloret, F., & Pons, X. (2003). Influence of fire severity on plant regeneration by means of remote sensing imagery. *International Journal of Remote Sensing*, *24*, 1751–1763.

Earl, N., & Simmonds, I. (2018). Spatial and temporal variability and trends in 2001-2016 global fire activity. *Journal of Geophysical Research: Atmospheres*, *123*, 2524–2536. https://doi.org/10.1002/2017JD027749

Fornacca, D., Ren, G., & Xiao, W. (2017). Performance of three MODIS fire products (MCD45A1, MCD64A1, MCD14ML), and ESA fire_CCI in a mountainous area of Northwest Yunnan, China, characterized by frequent small fires. *Remote Sensing*, *9*(11), 1131. https://doi.org/10.3390/rs9111131

Giglio, L., Boschetti, L., Roy, D. P., Humber, M. L., & Justice, C. O. (2018). The Collection 6 MODIS burned area mapping algorithm and product. *Remote Sensing of Environment*, *217*, 72–85.

Giglio, L., Schroeder, W., & Justice, C. O. (2016). The collection 6 MODIS active fire detection algorithm and fire products. *Remote Sensing of Environment*, *178*, 31–41.

Hernandez, C., Keribin, C., Drobinski, P., & Turquety, S. (2015). Statistical modelling of wildfire size and intensity: A step toward meteorological forecasting of summer extreme fire risk. *Annales Geophysicae*, *33*(12), 1495–1506.

Laurent, P., Mouillot, F., Moreno, M. V., Yue, C., & Ciais, P. (2019). Varying relationships between fire radiative power and fire size at a global scale. *Biogeosciences*, *16*(2), 275–288.

Lee, B., Kim, S. Y., Chung, J., & Park, P. S. (2008). Estimation of fire severity by use of Landsat TM images and its relevance to vegetation and topography in the 2000 Samcheok forest fire. *Journal of Forest Research*, *13*, 197–204.

Rossato, L., Alvala, R. C. S., Ferreira, N. J., & Tomasella, J. (2005). Evapotranspiration estimation in the Brazil using NDVI data. *Proceedings of SPIE*, *5976*, 377–385.

Sparks, A. M., Kolden, C. A., Smith, A. M. S., Boschetti, L., Johnson, D. M., & Cochrane, M. A. (2018). Fire intensity impacts on post-fire temperate coniferous forest net primary productivity. *Biogeosciences*, *15*(4), 1173–1183.

Wan, Z. (2008). New refinements and validation of the MODIS land-surface temperature/emissivity products. *Remote Sensing of Environment*, *112*(1), 59–74.